Developmental Cell, Volume *56*

Supplemental Information

ORF3a of the COVID-19 virus SARS-CoV-2 blocks HOPS complex-mediated assembly of the SNARE complex required for autolysosome formation

Guangyan Miao, Hongyu Zhao, Yan Li, Mingming Ji, Yong Chen, Yi Shi, Yuhai Bi, Peihui Wang, and Hong Zhang

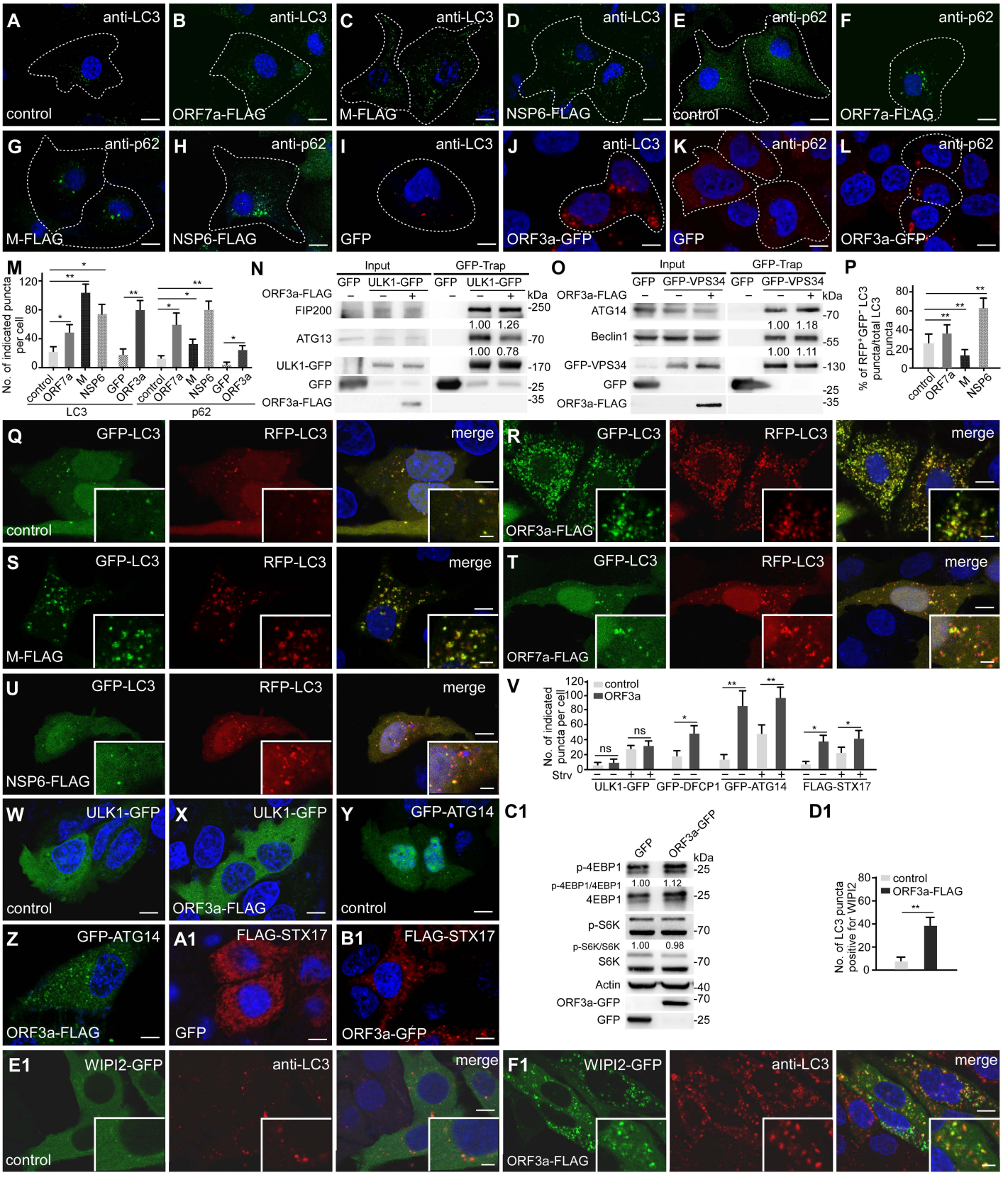
A anti-LC3 control
B anti-LC3 ORF7a-FLAG
C anti-LC3 M-FLAG
D anti-LC3 NSP6-FLAG
E anti-p62 control
F anti-p62 ORF7a-FLAG
G anti-p62 M-FLAG
H anti-p62 NSP6-FLAG
I anti-LC3 GFP
J anti-LC3 ORF3a-GFP
K anti-p62 GFP
L anti-p62 ORF3a-GFP
M No. of indicated puncta per cell
control ORF7a M NSP6 GFP ORF3a
LC3 p62
N Input GFP-Trap GFP ULK1-GFP
ORF3a-FLAG FIP200 ATG13 ULK1-GFP GFP ORF3a-FLAG kDa
1.00 1.26 1.00 0.78
O Input GFP-Trap GFP GFP-VPS34
ORF3a-FLAG ATG14 Beclin1 GFP-VPS34 GFP ORF3a-FLAG kDa
1.00 1.18 1.00 1.11
P % of RFP+GFP- LC3 puncta/total LC3 puncta
control ORF7a M NSP6
Q GFP-LC3 RFP-LC3 merge control
R GFP-LC3 RFP-LC3 merge ORF3a-FLAG
S GFP-LC3 RFP-LC3 merge M-FLAG
T GFP-LC3 RFP-LC3 merge ORF7a-FLAG
U GFP-LC3 RFP-LC3 merge NSP6-FLAG
V No. of indicated puncta per cell
control ORF3a
Strv ULK1-GFP GFP-DFCP1 GFP-ATG14 FLAG-STX17
W ULK1-GFP control
X ULK1-GFP ORF3a-FLAG
Y GFP-ATG14 control
Z GFP-ATG14 ORF3a-FLAG
A1 FLAG-STX17 GFP
B1 FLAG-STX17 ORF3a-GFP
C1 GFP ORF3a-GFP kDa
p-4EBP1 p-4EBP1/4EBP1 4EBP1 p-S6K p-S6K/S6K S6K Actin ORF3a-GFP GFP
1.00 1.12 1.00 0.98
D1 No. of LC3 puncta positive for WIPI2
control ORF3a-FLAG
E1 WIPI2-GFP anti-LC3 merge control
F1 WIPI2-GFP anti-LC3 merge ORF3a-FLAG

Figure S1

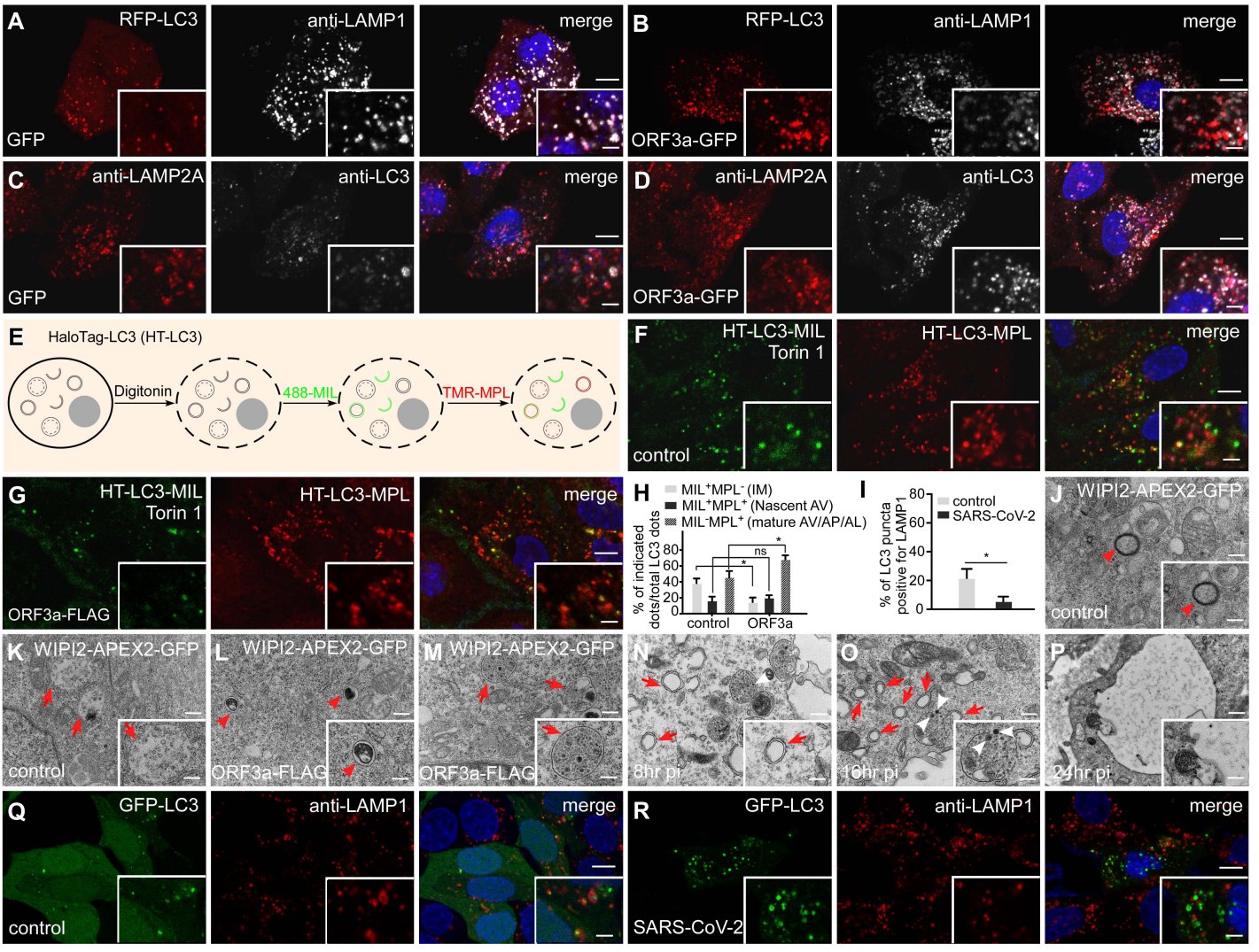
A
RFP-LC3
anti-LAMP1
merge
GFP
B
RFP-LC3
anti-LAMP1
merge
ORF3a-GFP
C
anti-LAMP2A
anti-LC3
merge
GFP
D
anti-LAMP2A
anti-LC3
merge
ORF3a-GFP
E
HaloTag-LC3 (HT-LC3)
Digitonin
488-MIL
TMR-MPL
F
HT-LC3-MIL
Torin 1
HT-LC3-MPL
merge
control
G
HT-LC3-MIL
Torin 1
HT-LC3-MPL
merge
ORF3a-FLAG
H
MIL+MPL- (IM)
MIL+MPL+ (Nascent AV)
MIL-MPL+ (mature AV/AP/AL)
% of indicated dots/total LC3 dots
ns
control
ORF3a
I
control
SARS-CoV-2
% of LC3 puncta positive for LAMP1
J
WIPI2-APEX2-GFP
control
K
WIPI2-APEX2-GFP
control
L
WIPI2-APEX2-GFP
ORF3a-FLAG
M
WIPI2-APEX2-GFP
ORF3a-FLAG
N
8hr pi
O
16hr pi
P
24hr pi
Q
GFP-LC3
anti-LAMP1
merge
control
R
GFP-LC3
anti-LAMP1
merge
SARS-CoV-2

Figure S2

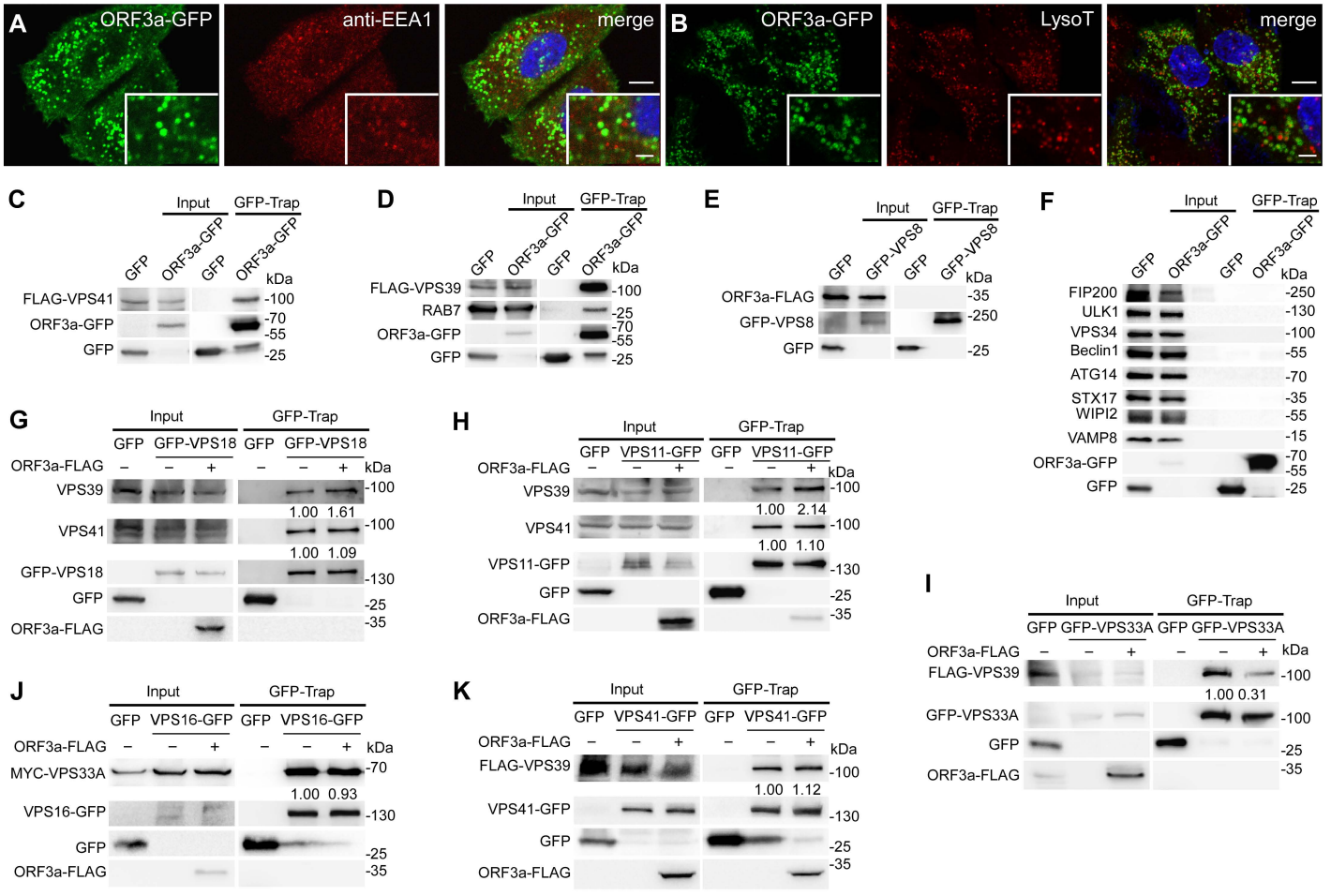
A
ORF3a-GFP
anti-EEA1
merge
B
ORF3a-GFP
LysoT
merge
C
Input
GFP-Trap
GFP
ORF3a-GFP
GFP
ORF3a-GFP
kDa
FLAG-VPS41
ORF3a-GFP
GFP
-100
-70
-55
-25
D
Input
GFP-Trap
GFP
ORF3a-GFP
GFP
ORF3a-GFP
kDa
FLAG-VPS39
RAB7
ORF3a-GFP
GFP
-100
-25
-70
-55
-25
E
Input
GFP-Trap
GFP
GFP-VPS8
GFP
GFP-VPS8
kDa
ORF3a-FLAG
GFP-VPS8
GFP
-35
-250
-25
F
Input
GFP-Trap
GFP
ORF3a-GFP
GFP
ORF3a-GFP
kDa
FIP200
ULK1
VPS34
Beclin1
ATG14
STX17
WIPI2
VAMP8
ORF3a-GFP
GFP
-250
-130
-100
-55
-70
-35
-55
-15
-70
-55
-25
G
Input
GFP-Trap
GFP
GFP-VPS18
GFP
GFP-VPS18
ORF3a-FLAG
–
–
+
–
–
+
kDa
VPS39
VPS41
GFP-VPS18
GFP
ORF3a-FLAG
1.00
1.61
1.00
1.09
-100
-100
-130
-25
-35
H
Input
GFP-Trap
GFP
VPS11-GFP
GFP
VPS11-GFP
ORF3a-FLAG
–
–
+
–
–
+
kDa
VPS39
VPS41
VPS11-GFP
GFP
ORF3a-FLAG
1.00
2.14
1.00
1.10
-100
-100
-130
-25
-35
I
Input
GFP-Trap
GFP
GFP-VPS33A
GFP
GFP-VPS33A
ORF3a-FLAG
–
–
+
–
–
+
kDa
FLAG-VPS39
GFP-VPS33A
GFP
ORF3a-FLAG
1.00
0.31
-100
-100
-25
-35
J
Input
GFP-Trap
GFP
VPS16-GFP
GFP
VPS16-GFP
ORF3a-FLAG
–
–
+
–
–
+
kDa
MYC-VPS33A
VPS16-GFP
GFP
ORF3a-FLAG
1.00
0.93
-70
-130
-25
-35
K
Input
GFP-Trap
GFP
VPS41-GFP
GFP
VPS41-GFP
ORF3a-FLAG
–
–
+
–
–
+
kDa
FLAG-VPS39
VPS41-GFP
GFP
ORF3a-FLAG
1.00
1.12
-100
-130
-25
-35

Figure S3

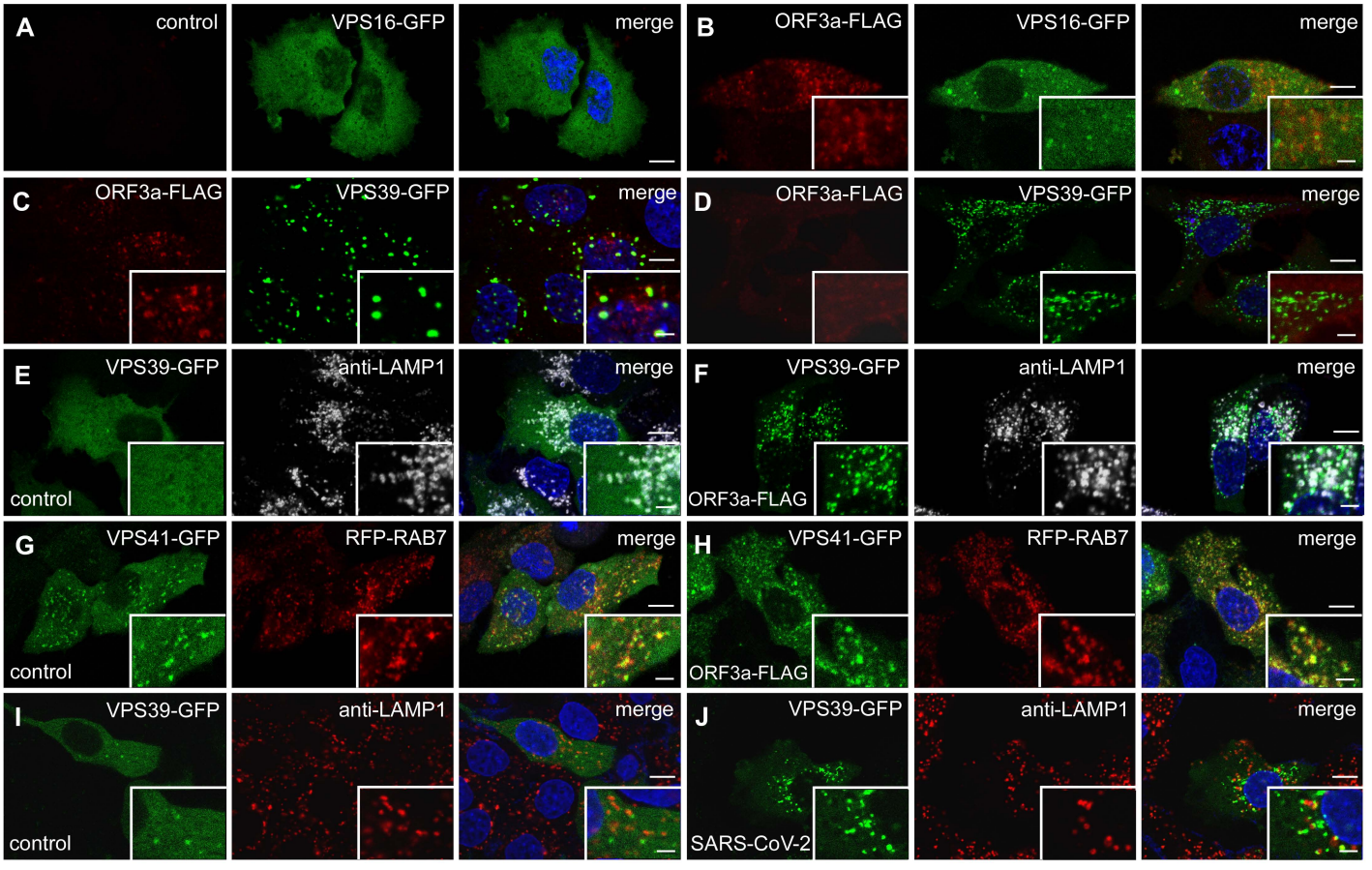
A
control
VPS16-GFP
merge
B
ORF3a-FLAG
VPS16-GFP
merge
C
ORF3a-FLAG
VPS39-GFP
merge
D
ORF3a-FLAG
VPS39-GFP
merge
E
VPS39-GFP
control
anti-LAMP1
merge
F
VPS39-GFP
ORF3a-FLAG
anti-LAMP1
merge
G
VPS41-GFP
control
RFP-RAB7
merge
H
VPS41-GFP
ORF3a-FLAG
RFP-RAB7
merge
I
VPS39-GFP
control
anti-LAMP1
merge
J
VPS39-GFP
SARS-CoV-2
anti-LAMP1
merge

Figure S4

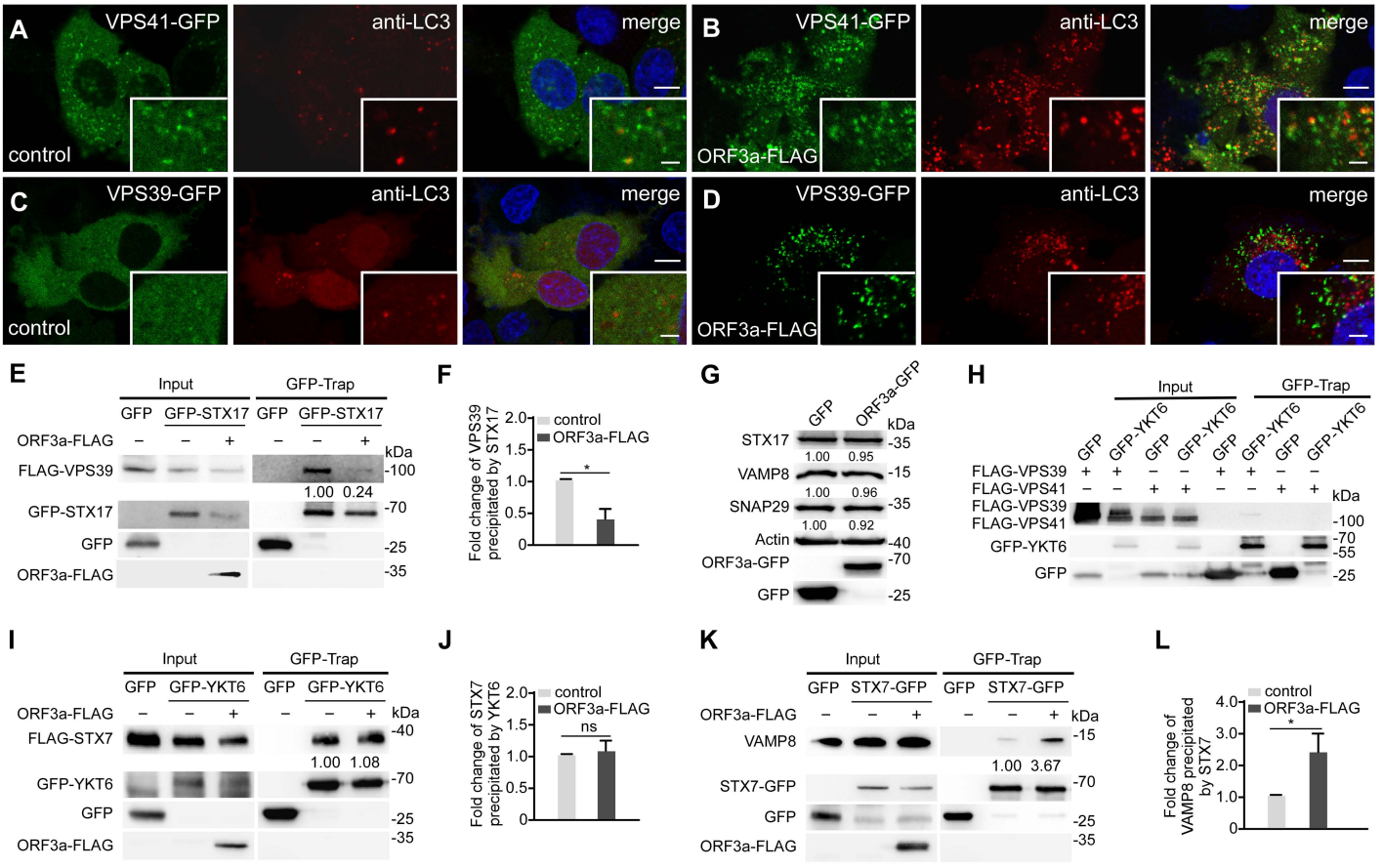
A
VPS41-GFP
anti-LC3
merge
control
B
VPS41-GFP
anti-LC3
merge
ORF3a-FLAG
C
VPS39-GFP
anti-LC3
merge
control
D
VPS39-GFP
anti-LC3
merge
ORF3a-FLAG
E
Input
GFP-Trap
GFP
GFP-STX17
ORF3a-FLAG
FLAG-VPS39
GFP-STX17
GFP
ORF3a-FLAG
kDa
-100
-70
-25
-35
1.00 0.24
F
Fold change of VPS39 precipitated by STX17
control
ORF3a-FLAG
*
G
GFP
ORF3a-GFP
kDa
STX17
VAMP8
SNAP29
Actin
ORF3a-GFP
GFP
-35
-15
-35
-40
-70
-25
1.00 0.95
1.00 0.96
1.00 0.92
H
Input
GFP-Trap
GFP
GFP-YKT6
FLAG-VPS39
FLAG-VPS41
GFP-YKT6
GFP
kDa
-100
-70
-55
-25
I
Input
GFP-Trap
GFP
GFP-YKT6
ORF3a-FLAG
FLAG-STX7
GFP-YKT6
GFP
ORF3a-FLAG
kDa
-40
-70
-25
-35
1.00 1.08
J
Fold change of STX7 precipitated by YKT6
control
ORF3a-FLAG
ns
K
Input
GFP-Trap
GFP
STX7-GFP
ORF3a-FLAG
VAMP8
STX7-GFP
GFP
ORF3a-FLAG
kDa
-15
-70
-25
-35
1.00 3.67
L
Fold change of VAMP8 precipitated by STX7
control
ORF3a-FLAG
*

Figure S5

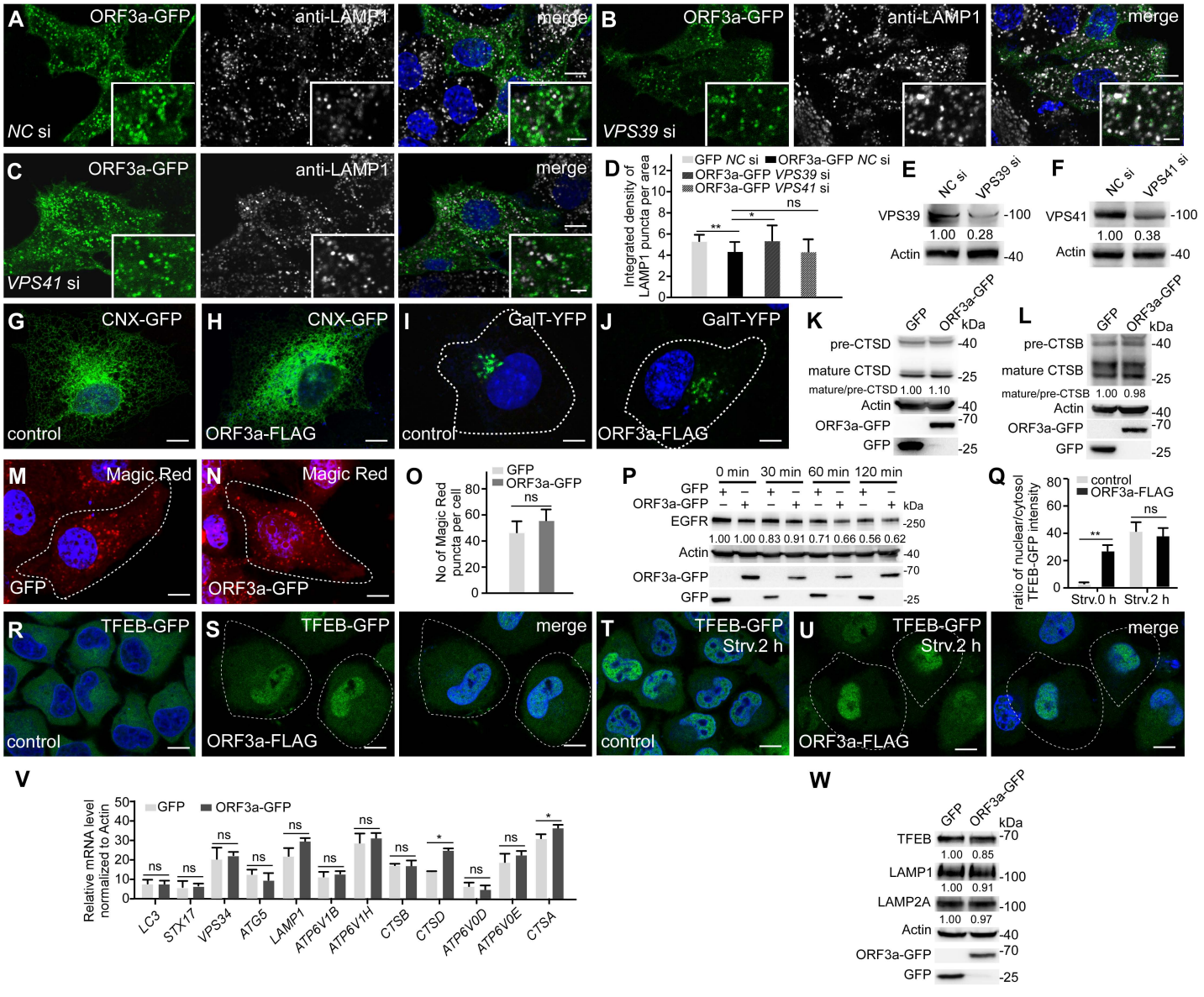
A
ORF3a-GFP
anti-LAMP1
merge
NC si
B
VPS39 si
C
VPS41 si
D
GFP NC si
ORF3a-GFP NC si
ORF3a-GFP VPS39 si
ORF3a-GFP VPS41 si
Integrated density of LAMP1 puncta per area
ns
E
NC si
VPS39 si
VPS39
1.00 0.28
Actin
F
VPS41
1.00 0.38
G
CNX-GFP
control
H
ORF3a-FLAG
I
GalT-YFP
J
K
GFP
ORF3a-GFP
kDa
pre-CTSD
mature CTSD
mature/pre-CTSD 1.00 1.10
ORF3a-GFP
L
pre-CTSB
mature CTSB
mature/pre-CTSB 1.00 0.98
M
Magic Red
N
O
No of Magic Red puncta per cell
P
0 min
30 min
60 min
120 min
EGFR
1.00 1.00 0.83 0.91 0.71 0.66 0.56 0.62
Q
control
ORF3a-FLAG
ratio of nuclear/cytosol TFEB-GFP intensity
Strv.0 h
Strv.2 h
R
TFEB-GFP
S
T
Strv.2 h
U
V
Relative mRNA level normalized to Actin
LC3
STX17
VPS34
ATG5
LAMP1
ATP6V1B
ATP6V1H
CTSB
CTSD
ATP6V0D
ATP6V0E
CTSA
W
TFEB
1.00 0.85
LAMP1
1.00 0.91
LAMP2A
1.00 0.97

Figure S6

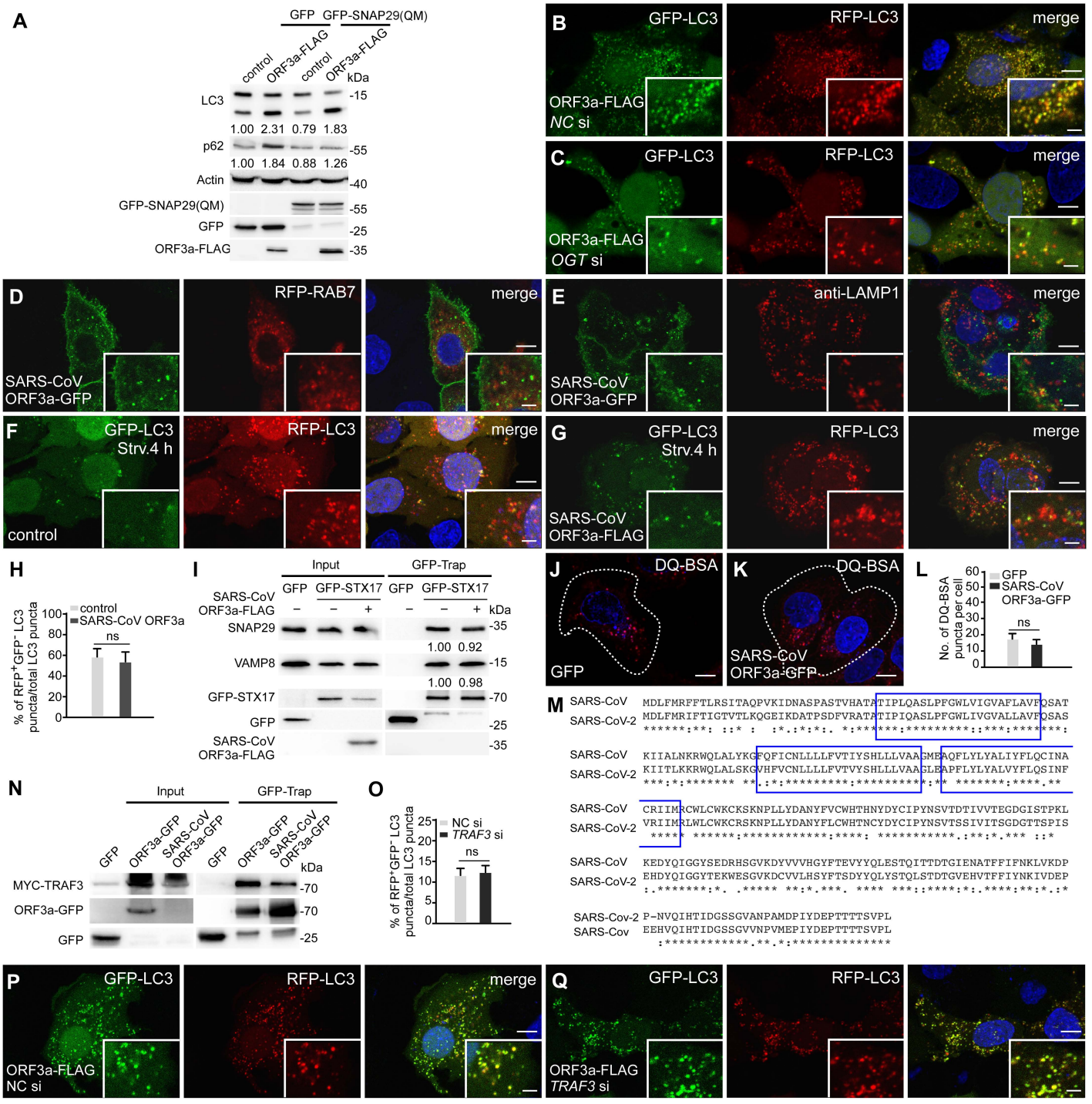
A
GFP
GFP-SNAP29(QM)
control
ORF3a-FLAG
control
ORF3a-FLAG
kDa
LC3
-15
1.00 2.31 0.79 1.83
p62
-55
1.00 1.84 0.88 1.26
Actin
-40
GFP-SNAP29(QM)
-55
GFP
-25
ORF3a-FLAG
-35
B
GFP-LC3
RFP-LC3
merge
ORF3a-FLAG
NC si
C
GFP-LC3
RFP-LC3
merge
ORF3a-FLAG
OGT si
D
RFP-RAB7
merge
SARS-CoV
ORF3a-GFP
E
anti-LAMP1
merge
SARS-CoV
ORF3a-GFP
F
GFP-LC3
Strv.4 h
RFP-LC3
merge
control
G
GFP-LC3
Strv.4 h
RFP-LC3
merge
SARS-CoV
ORF3a-FLAG
H
control
SARS-CoV ORF3a
% of RFP+GFP- LC3 puncta/total LC3 puncta
ns
I
Input
GFP-Trap
SARS-CoV
ORF3a-FLAG
GFP
GFP-STX17
GFP
GFP-STX17
kDa
SNAP29
-35
1.00 0.92
VAMP8
-15
1.00 0.98
GFP-STX17
-70
GFP
-25
SARS-CoV
ORF3a-FLAG
-35
J
DQ-BSA
GFP
K
DQ-BSA
SARS-CoV
ORF3a-GFP
L
GFP
SARS-CoV
ORF3a-GFP
No. of DQ-BSA puncta per cell
ns
M
SARS-CoV
SARS-CoV-2
N
Input
GFP-Trap
GFP
ORF3a-GFP
SARS-CoV
ORF3a-GFP
GFP
ORF3a-GFP
SARS-CoV
ORF3a-GFP
kDa
MYC-TRAF3
-70
ORF3a-GFP
-70
GFP
-25
O
NC si
TRAF3 si
% of RFP+GFP- LC3 puncta/total LC3 puncta
ns
P
GFP-LC3
RFP-LC3
merge
ORF3a-FLAG
NC si
Q
GFP-LC3
RFP-LC3
ORF3a-FLAG
TRAF3 si

Figure S7

SUPPLEMENTAL ITEM

Table S1. List of oligonucleotides used in this study (related to STAR METHODS: Key Resources Table)

REAGENT or RESOURCE	SOURCE	IDENTIFIER
Oligonucleotides		
RT primers for human *Actin* (5'-3') F: TGGCTCCTAGCACCATGAAGAT R: GGTGGACAGTGAGGCCAGGAT	This paper	N/A
RT primers for human *ATP6V1H* (5'-3') F: GGAAGTGTCAGATGATCCCCA R: CCGTTTGCCTCGTGGATAAT	This paper	N/A
RT primers for human *CTSB* (5'-3') F: AGTGGAGAATGGCACACCCTA R: AAGAAGCCATTGTCACCCCA	This paper	N/A
RT primers for human *CTSD* (5'-3') F: AACTGCTGGACATCGCTTGCT R: CATTCTTCACGTAGGTGCTGGA	This paper	N/A
RT primers for human *CTSA* (5'-3') F: CAGGCTTTGGTCTTCTCTCCA R: TCACGCATTCCAGGTCTTTG	This paper	N/A
RT primers for human *ATP6V0D2* (5'-3') F: CATTCTTGAGTTTGAGGCCG R: CCGTAATGATCCGCTACGTT	This paper	N/A
RT primers for human *ATP6V1B2* (5'-3') F: GAGGGGCAGATCTATGTGGA R: GCATGATCCTTCCTGGTCAT	This paper	N/A
RT primers for human *ATP6V0E1* (5'-3') F: CATTGTGATGAGCGTGTTCTGG R: AACTCCCCGGTTAGGACCCTTA	This paper	N/A
RT primers for human *LC3* (5'-3') F: GAGAAGACCTTCAAGCAG R: GAGGCATAGACCATGTACAG	This paper	N/A
RT primers for human *LAMP1* (5'-3') F: ACGTTACAGCGTCCAGCTCAT R: TCTTTGGAGCTCGCATTGG	This paper	N/A
RT primers for human *STX17* (5'-3') F: GCAGAATCTGGGACAAGTTG R: CTCTGAGAACTAGCTTCAGC	This paper	N/A
RT primers for human *VPS34* (5'-3') F: CTTGGAAGGGAAGAGAGAAC R: GAGCGAAACCGTTGTTCCTC	This paper	N/A
RT primers for human *ATG5* (5'-3') F: GAAGGAGGAGCCATAGCTTG R: CATTTCAGTGGTGTGCCTTC	This paper	N/A

Supplementary Figure Legends

Table S1. List of oligonucleotides used in this study (related to STAR METHODS: Key Resources Table)

Supplementary Figure 1. Expression of ORF3a inhibits autophagy activity, related to Figure 1.

(**A**-**H**) Immunostaining with anti-LC3 and anti-p62 antibodies shows the accumulation of LC3 and p62 puncta in HeLa cells expressing of ORF7a-FLAG (B and F), M-FLAG (C and G) and NSP6-FLAG (D and H). Cells transfected with FLAG-expressing constructs were used as controls (A and E). The cells expressing the corresponding genes are outlined. Scale bars: 5 μm.

(**I**-**L**) Compared with control HEK-293T cells (I and K), expression of ORF3a-GFP induces more LC3 and p62 puncta (J and L). Scale bars: 10 μm.

(**M**) Quantification of the numbers of LC3 and p62 puncta shown in (A-L). Data are shown as mean ± SEM (n =25 cells in each group). LC3 and p62 puncta were examined in HeLa cells expressing ORF7a, M and NSP6 and HEK-293T cells expressing ORF3a. *, $p<0.05$; **, $p<0.01$.

(**N**) The levels of endogenous FIP200 and ATG13 precipitated by ULK1-GFP in GFP-Trap assays in control cells and cells expressing ORF3a-FLAG. Quantification of FIP200 and ATG13 levels (normalized by ULK1-GFP levels) is also shown.

(**O**) Levels of endogenous ATG14 and Beclin1 precipitated by GFP-VPS34 in

GFP-Trap assays are slightly increased in ORF3a-FLAG-expressing cells compared to control cells. Quantification of ATG14 and Beclin1 levels (normalized by GFP-VPS34 levels) is also shown.

(**P**) Quantification of the percentage of $RFP^{+}GFP^{-}$LC3 puncta among total LC3 puncta in control, ORF7a-FLAG, M-FLAG and NSP6-FLAG-expressing cells. Data are shown as mean ± S.E.M. (n =18 cells in each group). **p<0.01.

(**Q** and **R**) Compared with control cells (Q), cells expressing ORF3a-FLAG contain many more LC3 puncta that are positive for both RFP and GFP (R) under normal conditions. Scale bars: 5 μm; inserts, 2 μm.

(**S-U**) Cells expressing of M-FLAG contain more LC3 puncta that are positive for both RFP and GFP (S), while in cells expressing ORF7a-FLAG (T) or NSP6-FLAG (U), a large number of red-only LC3 puncta accumulate under normal conditions. Scale bars: 5 μm; inserts, 2 μm.

(**V**) Quantification of the numbers of indicated puncta is shown as mean ± SEM. (n =24 cells in each group). ns: no significant difference. *, p<0.05; **, p<0.01.

(**W** and **X**) ULK1-GFP shows no obvious change in control cells (W) and ORF3a-FLAG-expressing cells (X) under nutrient-rich conditions. Scale bars: 5 μm.

(**Y** and **Z**) Compared with control cells (Y), GFP-ATG14 forms more punctate structures in ORF3a-FLAG-expressing cells under nutrient-rich conditions (Z). Scale bars: 5 μm.

(**A1** and **B1**) Compared with control cells (A1), FLAG-STX17 forms more punctate

structures in ORF3a-GFP-expressing cells under nutrient-rich conditions (B1). Scale bars: 5 μm.

(**C1**) Immunoblotting assays showing that compared to control cells, levels of p-4EBP1/4EBP1 and p-S6K/S6K are not obviously changed in cells expressing ORF3a-GFP under nutrient-rich conditions. Levels of p-4EBP1/4EBP1 and p-S6K /S6K are normalized by Actin and set to 1.00 in control cells.

(**D1**) Quantification of the number of LC3 puncta co-localizing with WIPI2 puncta in control and ORF3a-GFP-expressing cells. Data are shown as mean ± S.E.M. (n =20 cells in each group). **p<0.01.

(**E1** and **F1**) Compared with control cells (E1), WIPI2-GFP forms more punctate structures that colocalize with LC3 puncta in ORF3a-FLAG-expressing cells. Scale bars: 5 μm; inserts, 2 μm.

Supplementary Figure 2. Expression of ORF3a or SARS-CoV-2 infection blocks autophagosome maturation, related to Figure 1 and Figure 2.

(**A** and **B**) In ORF3a-GFP-expressing cells, a smaller percentage of LC3 puncta co-localize with LAMP1-labeled late endosome/lysosomes (B) than in control cells (A). Scale bars: 5 μm; inserts, 2 μm.

(**C** and **D**) In ORF3a-GFP-expressing cells, a smaller percentage of LC3 puncta co-localize with LAMP2A-labeled lysosomes (D) than in control cells (C). Scale bars: 5 μm; inserts, 2 μm.

(**E)** Schematic illustration of the HaloTag-LC3 assay. After permeabilization with

digitonin, cells expressing HaloTag-LC3 are stained with the membrane-impermeable Halo ligand (MIL) HaloTag® Alexa Fluor® 488. HaloTag-LC3 on the isolation membranes (IMs) and the outer membrane of nascent autophagosomes is labeled in green. Then cells are fixed and stained with the membrane-permeable Halo ligand (MPL) HaloTag® TMR, and Halo-LC3 inside autophagosomes, amphisomes and autolysosomes is labeled in red.

(**F**-**H**) In HaloTag-LC3 assays, after 1 h Torin 1 treatment, both MIL^+ HaloTag-LC3 puncta and MPL^+ HaloTag-LC3 puncta are formed in control cells (F), while in ORF3a-expressing cells, most of the HaloTag-LC3 puncta are MIL^-MPL^+ (G). IM, isolation membrane. AV, autophagosome. AP, amphisome. AL, autolysosomes. Quantification of the percentages of MIL^+MPL^- (IMs), MIL^+MPL^+ (nascent autophagosomes) and MIL^-MPL^+ (mature autophagosomes/amphisomes/autolysosomes) HaloTag-LC3 puncta are shown in (H) as mean ± SEM (n =20 cells in each group). ns: no significant difference; *, $p<0.05$. Scale bars: 5 μm; inserts, 2 μm.

(**I**) Quantification of the percentage of LC3 puncta co-localizing with LAMP1 puncta in control and SARS-CoV-2-infected cells. Data are shown as mean ± S.E.M. (n =18 cells in each group). *, $p<0.05$.

(**J**-**M**) EM analysis in cells transfected with WIPI2-APEX2-GFP indicates that APEX2-derived dark signal is present on closed nascent autophagosomes (red arrowheads) in control cells treated with Bafilomycin A1, but not on

amphisomes (red arrows) (J and K). In ORF3a-expressing cells (L and M), dark WIPI2-APEX2 signals were detected on membranes of autophagosomes (red arrowheads) and amphisomes (red arrows). Scale bars: 0.5 μm; inserts, 0.2 μm.

(**N-P**) EM analysis indicates that double-membrane vesicles (DMVs) (red arrows) accumulate in SARS-CoV-2-infected cells at 8 hr pi (N), 16 hr pi (O) and 24 hr pi (P). The white arrowheads indicate virion particles. The diameter of DMVs is about 301±82 nm (n=71) in SARS-CoV-2-infected cells. Scale bars: 0.5 μm; inserts, 0.2 μm.

(**Q** and **R**) In SARS-CoV-2-infected cells, far fewer LC3 puncta co-localize with LAMP1-labeled lysosomes (R) than in control cells (Q). Scale bars: 5 μm; inserts, 2 μm.

Supplementary Figure 3. ORF3a interacts with components of the HOPS complex, related to Figure 3.

(**A**) ORF3a-GFP puncta are separate from EEA1-labeled early endosomes in HeLa cells. Scale bars: 5 μm; inserts, 2 μm.

(**B**) ORF3a-GFP puncta partially colocalize with LysoTracker-stained lysosomes. LysoT: LysoTracker. Scale bars: 5 μm; inserts, 2 μm.

(**C**) FLAG-VPS41 is co-immunoprecipitated by ORF3a-GFP in GFP-Trap assays.

(**D**) FLAG-VPS39 and endogenous RAB7 are co-immunoprecipitated by ORF3a-GFP in GFP-Trap assays.

(**E**) In GFP-Trap assays, ORF3a-FLAG fails to be precipitated by GFP-VPS8.

(**F**) In GFP-Trap assays, endogenous FIP200, ULK1, VPS34, ATG14, Beclin1, STX17, WIPI2 and VAMP8 fail to be co-precipitated by ORF3a-GFP.

(**G**) In GFP-Trap assays, levels of endogenous VPS39 precipitated by GFP-VPS18 are higher in ORF3a-FLAG-expressing cells than control cells, while levels of endogenous VPS41 precipitated by GFP-VPS18 show no obvious change. Quantification of VPS39 and VPS41 levels (normalized by GFP-VPS18 level) is also shown.

(**H**) In GFP-Trap assays, levels of endogenous VPS39 precipitated by VPS11-GFP are increased, while levels of endogenous VPS41 precipitated by VPS11-GFP show no obvious change in ORF3a-FLAG-expressing cells compared to control cells. Quantification of VPS339 and VPS41 levels (normalized by VPS11-GFP level) is also shown.

(**I**) In GFP-Trap assays, levels of FLAG-VPS39 precipitated by GFP-VPS33A are lower in ORF3a-FLAG-expressing cells than control cells. Quantification of FLAG-VPS39 level (normalized by GFP-VPS33A level) is also shown.

(**J**) In GFP-Trap assays, levels of Myc-tagged VPS33A precipitated by VPS16-GFP show no obvious change in ORF3a-FLAG-expressing cells compared to control cells. Quantification of Myc-VPS33A level (normalized by VPS16-GFP level) is also shown.

(**K**) In GFP-Trap assays, levels of FLAG-VPS39 precipitated by VPS41-GFP show no obvious change in ORF3a-FLAG-expressing cells compared to control cells. Quantification of FLAG-VPS39 level (normalized by VPS41-GFP level) is also

shown.

Supplementary Figure 4. ORF3a or SARS-CoV-2 infection sequestrates VPS39 on late endosomes, related to Figure 3.

(**A** and **B**) Compared with control cells (A), VPS16-GFP forms more punctate structures that colocalize with ORF3a-FLAG (B) in ORF3a-FLAG-expressing cells. Scale bars: 5 μm; inserts, 2 μm.

(**C** and **D**) When co-transfected with ORF3a-FLAG, VPS39-GFP forms several large puncta that co-localize with ORF3a-FLAG (C) in some cells. Even in cells with a very low ORF3a-FLAG level, VPS39-GFP still forms many small punctate structures (D). Scale bars: 5 μm; inserts, 2 μm.

(**E** and **F**) VPS39-GFP punctate structures largely colocalize with LAMP1-labeled late endosomes/lysosomes in cells expressing ORF3a-FLAG (F). VPS39-GFP is diffusely localized in control cells (E). Scale bars: 5 μm; inserts, 2 μm.

(**G** and **H**) VPS41-GFP punctate structures colocalize with RFP-RAB7-labeled late endosomes in control cells (G) and cells expressing ORF3a-FLAG (H). Scale bars: 5 μm; inserts, 2 μm.

(**I** and **J**) Compared to control cells (I), VPS39-GFP forms many more punctate structures that partially colocalize or closely associate with LAMP1-labeled lysosomes in SARS-CoV-2-infected cells (J). Scale bars: 5 μm; inserts, 2 μm.

Supplementary Figure 5. ORF3a inhibits the formation of the

STX17-SNAP29-VAMP8 complex, related to Figure 4.

(**A** and **B**) Compared to control cells (A), fewer VPS41-GFP punctate structures colocalize with LC3 puncta in cells expressing ORF3a-FLAG (B). Scale bars: 5 μm; inserts, 2 μm.

(**C** and **D**) In control cells (C), VPS39-GFP is diffusely localized, while in cells expressing of ORF3a-FLAG (D), VPS39-GFP forms a large number of punctate structures that are separate from LC3-labeled puncta. Scale bars: 5 μm; inserts, 2 μm.

(**E**) In GFP-Trap assays, levels of FLAG-VPS39 precipitated by GFP-STX17 are decreased in ORF3a-FLAG-expressing cells compared to control cells. Quantification of FLAG-VPS39 level (normalized by GFP-STX17 level) is also shown.

(**F**) Quantification of the fold change of VPS39 level precipitated by STX17 in control cells and ORF3a-expressing cells is shown as mean ± S.E.M. Results are representative of at least three experiments. *$p<0.05$.

(**G**) Immunoblotting assays showing that levels of STX17, VAMP8 and SNAP29 are not obviously changed in cells expressing ORF3a-GFP. Levels of STX17, VAMP8 and SNAP29 are normalized by Actin and set to 1.00 in control cells.

(**H**) FLAG-VPS39 and FLAG-VPS41 fail to be co-immunoprecipitated by GFP-YKT6 in GFP-Trap assays.

(**I**) In GFP-Trap assays, levels of FLAG-STX7 precipitated by GFP-YKT6 show no obvious change in ORF3a-FLAG-expressing cells compared to control cells.

Quantification of FLAG-STX7 level (normalized by GFP-YKT6 level) is also shown.

(**J**) Quantification of the fold change of STX7 level precipitated by YKT6 in control cells and ORF3a-expressing cells is shown as mean ± S.E.M. Results are representative of at least three experiments. ns: no significant difference.

(**K**) In GFP-Trap assays, levels of endogenous VAMP8 precipitated by STX7-GFP are higher in ORF3a-FLAG-expressing cells than control cells. Quantification of VAMP8 level (normalized by STX7-GFP level) is also shown.

(**L**) Quantification of the fold change of VAMP8 level precipitated by STX7 in control cells and ORF3a-expressing cells is shown as mean ± S.E.M. Results are representative of at least three experiments. *$p<0.05$.

Supplementary Figure 6. ORF3a affects late endosomal/lysosomal biogenesis and induces lysosomal damage, related to Figure 5.

(**A**-**D**) In control siRNA-treated cells (A), ORF3a-GFP forms many punctate structures that partially colocalize with LAMP1-labeled late endosomes/lysosomes. In cells treated by *VPS39* siRNA (B), ORF3a-GFP forms smaller and fewer punctate structures that still partially colocalize with LAMP1-labeled structures. In ORF3a-expressing cells, the intensity of anti-LAMP1 signal is increased by *VPS39* KD. *VPS41* KD fails to alter the number or size of ORF3a-GFP punctate structures and does not restore the staining intensity of LAMP1 signal in ORF3a-expressing cells (C). Quantification

of the integrated density of LAMP1 puncta per area in (D) is shown as mean ± S.E.M. (n =22 cells in each group). ns: no significant difference, *p<0.05, **p<0.01. NC, negative control. Scale bars: 5 μm; inserts, 2 μm.

(**E**) Protein level of VPS39 is dramatically reduced in *VPS39* siRNA-treated cells. Level of VPS39 is normalized by Actin and set to 1.00 in control cells.

(**F**) Protein level of VPS41 is dramatically reduced in *VPS41* siRNA treated cells. Level of VPS41 is normalized by Actin and set to 1.00 in control cells.

(**G** and **H**) The pattern of Calnexin (CNX)-GFP-labeled ER structures is similar in control cells (G) and ORF3a-FLAG-expressing cells (H). Scale bars: 5 μm.

(**I** and **J**) The pattern of GalT-YFP-labeled trans-Golgi network is similar in control cells (I) and ORF3a-FLAG-expressing cells (J). Scale bars: 5 μm.

(**K**) Levels of the mature form of cathepsin D (CTSD) are similar in ORF3a-GFP-expressing cells and control cells. Quantification of the ratio of mature/pre-mature cathepsin D is also shown. Level of CTSD is normalized by Actin.

(**L**) Levels of the mature form of cathepsin B (CTSB) are similar in ORF3a-GFP-expressing cells and control cells. Quantification of the ratio of mature/pre-mature cathepsin B is also shown. Level of CTSB is normalized by Actin.

(**M-O**) The number of Magic Red-stained punctate structures in control (M) and ORF3a-GFP-expressing cells (N). Quantification data of the number of Magic Red-stained puncta in (O) are shown as mean ± S.E.M. (n =26 cells in each

group). ns: no significant difference. Scale bars: 5 μm.

(**P**) Degradation of EGFR in control and ORF3a-GFP-expressing cells at different time points. HeLa cells were deprived of EGF and serum overnight and stimulated with EGF in the presence of CHX for the indicated times in control cells and ORF3a-GFP-expressing cells. Levels of EGFR in each cell type at 0 min were set to 1.00.

(Q-U) In control HeLa cells stably expressing TFEB-GFP, TFEB-GFP is predominantly localized in the cytoplasm (R). TFEB-GFP is translocated into the nucleus following starvation treatment (T). In ORF3a-FLAG-expressing cells, TFEB-GFP is predominantly localized in the nucleus under nutrient-rich conditions (S) and starvation conditions (U). (Q) shows quantification of the ratio of nuclear TFEB-GFP/cytosolic TFEB-GFP measured by the fluorescence intensity. Data are shown as mean ± S.E.M. (n=30 cells in each group). ns: no significant difference; **, $p<0.01$.

(**V**) Transcriptional levels of genes involved in autophagy and lysosomal biogenesis, including *LC3*, *STX17*, *VPS34*, *ATG5*, *LAMP1*, *ATP6V1B*, *ATP6V1H*, *CTSB*, *ATP6V0D* and *ATP6V0E*, show no evident change, while mRNA levels of *CTSD* and *CTSA* are increased in ORF3a-FLAG-expressing cells compared to control cells. ns: no significant difference; *$p<0.05$. Data from three independent experiments were compared with two-tailed, unpaired Student's t-tests.

(**W**) Immunoblotting assays showing that levels of TFEB, LAMP1 and LAMP2A are

slightly decreased in cells expressing ORF3a-GFP. Levels of TFEB, LAMP1 and LAMP2A are normalized by Actin and set to 1.00 in control cells.

Supplementary Figure 7. SARS-CoV ORF3a fails to interact with the HOPS complex or affect autophagy, related to Figure 6.

(**A**) Levels of LC3 and p62 in control and ORF3a-FLAG-expressing cells transfected with control GFP and GFP-SNAP29(QM). SNAP29(QM) contains mutations at the four *O*-GlcNAcylated sites in SNAP29 (S2A, S61G, T130A and S153G). Levels of LC3-II and p62 levels are normalized by Actin and set to 1.00 in control cells.

(**B** and **C**) RFP-GFP-LC3 assays show that more $RFP^{+}GFP^{-}$LC3 puncta are detected in *siOGT*-treated ORF3a-expressing cells (C) compared to *siNC*-treated ORF3a-expressing cells (B) under nutrient-rich conditions. NC, negative control.

(**D** and **E**) SARS-CoV ORF3a-GFP localizes on the plasma membrane and also form some punctate structures that are separate from RAB7-labeled late endosomes (D) and LAMP1-labeled late endosomes/lysosomes (E). Scale bars: 5 μm; inserts, 2 μm.

(**F-H**) RFP-GFP-LC3 assays show that as in control cells (F), SARS-CoV ORF3a-FLAG-expressing cells (G) also contain a large number of $RFP^{+}GFP^{-}$LC3 puncta after 4 h starvation. (H) shows quantification of the percentage of $RFP^{+}GFP^{-}$LC3 puncta among total LC3 puncta in control and SARS-ORF3a-FLAG-expressing cells (mean ± S.E.M., n =27 cells in each

group). ns: no significant difference. Scale bars: 5 μm; inserts, 2 μm.

(**I**) Levels of endogenous SNAP29 and VAMP8 precipitated by GFP-STX17 are similar in control cells and SARS-CoV ORF3a-FLAG-expressing cells in GFP-Trap assays. Quantification of SNAP29 and VAMP8 levels (normalized by GFP-STX17 level) is also shown.

(**J**-**L**) Compared to control cells (J), the number of DQ-BSA-labeled punctate structures is not obviously changed in SARS-CoV ORF3a-GFP-expressing cells (K). Quantification of the number of DQ-BSA-labeled punctate structures in GFP control and SARS-CoV ORF3a-GFP-expressing cells is shown in (L) as mean ± S.E.M. (n =25 cells in each group). ns: no significant difference. Scale bars: 5 μm.

(**M**) Sequence alignment of ORF3a of SARS-Cov-2 and SARS-CoV with Clustal Omega. " * " indicates positions which have the same residue; " : " indicates conservation of amino acids with strongly similar properties-roughly equivalent to scoring > 0.5 in the Gonnet PAM 250 matrix; " . " indicates conservation of amino acids with weakly similar properties-roughly equivalent to scoring =< 0.5 and > 0 in the Gonnet PAM 250 matrix. The three transmembrane regions of ORF3a are indicated by blue boxes.

(**N**) In GFP-Trap assays, MYC-TRAF3 is precipitated by both SARS-CoV ORF3a-GFP and SARS-CoV-2 ORF3a-GFP.

(**O**-**Q**) RFP-GFP-LC3 assays show that the percentage of $RFP^{+}GFP^{-}$LC3 puncta is not obviously changed in *siTRAF3*-treated ORF3a-expressing cells (Q) compared to

control *siRNA*-treated ORF3a-expressing cells (P). Quantification data (n=15 cells in each group) are shown as mean ± SEM in (O). ns: no significant difference. Scale bars: 5 μm; inserts, 2 μm.